

## EFFECT OF REMELTING OF THE Ni-22Cr-9Mo ALLOY ON ITS MICROSTRUCTURAL AND ELECTROCHEMICAL PROPERTIES

The Ni-Cr-Mo alloys are used as the alternative for the cobalt alloys in the manufacture of metal prosthetic elements, i.e. crowns, bridges and frame prostheses. The article attempts at a materials science characterization of the nickel-based alloy of the commercial name Argeloy N.P Be-Free by Argen. Within the study, examinations were made on the commercial alloy as well as the alloy which was remelted and cast by the lost mould (lost wax) method. Observations of the microstructure were performed with the use of optical and electron scanning microscopy. Also, X-ray structural tests were conducted as well as corrosion resistance tests in an artificial saliva solution (pH = 6,7). It was demonstrated that the examined Ni-22Cr-9Mo alloy characterized in a dendritic structure typical of the cast materials. The X-ray qualitative phase analysis revealed the phase  $\gamma'$  (Ni) in both examined materials, as well as the presence of  $\text{Cr}_{23}\text{C}_6$  type carbides and  $\text{Nb}_2\text{C}$ ,  $\text{Ta}_2\text{C}$  (commercial alloy) and  $\text{NbC}$ ,  $\text{Ta}_4\text{C}_{0,04}$  (cast alloy) phases. The effect of the alloy's remelting and the morphology of the passive layer on the corrosion resistance of the Ni-Cr-Mo alloy was examined.

The results of the electrochemical tests show that the process of re-casting only slightly affects the corrosion resistance and the microstructure of the considered alloy.

The roles of recasting process and the passive film homogeneity on the corrosion resistance of Ni-Cr-Mo dental alloy were reviewed. The results of the electrochemical study show that the dependence of corrosion resistance on the microstructure associated with the recasting process is marginal.

*Keywords:* Ni-Cr-Mo alloys, metal prosthetics restorations, method melted models, artificial saliva solution, corrosion resistance

### 1. Introduction

The dynamic development of materials science for the purposes of stomatological prosthetics is directed towards restoring, improving and recreating the correct shape of the patient's anatomic dental system as well as the esthetic values of the tooth itself.

The dental technician replaces the patient's lost teeth with metal crowns etc. The materials which characterize in a good metal-ceramics joint are the Ni-Cr-Mo alloys.

The use of the Ni-Cr-Mo alloys mainly results from the facility in obtaining the required mechanical properties of the prosthetic elements, at a relatively low production cost. The chemical composition of the Ni casting alloys, according to the standard ISO 6871-2, mainly consists of 70-80% Ni and 10-25% Cr, as well as additions of Mo (min. 4%), W (min. 4%) or (more rarely) Be (max. 2%) [1]. The total content of Ni+Cr+Mo should equal the minimum of 85% wt.

The division of the nickel alloys results from the presence of beryllium in these materials. Beryllium's task is to improve the castability of the alloy by way of lowering the melting temperature, also, it affects the refinement of the grain and increases the hardness by forming the NiBe phase as an interdendritic compo-

nent of the eutectic mixture. Additionally, beryllium facilitates the oxidation of the metal surface, which positively affects the ceramics adhesion in the production of crowns. The main disadvantage of beryllium is its strong toxicity, as well as its contribution to crevice and pitting corrosion in the nickel alloys [2-5].

The nickel casting alloys, similarly to the cobalt alloys, characterize in a low thermal conductivity, which makes the patient insensitive to the sudden changes of the food temperature in the case of possessing dental crowns or bridges. They can also be used for partial removable reconstructions, including frame prostheses, in combination with other materials (ceramics, acrylic).

The prosthetic materials made of nickel alloys provide comfort to their user without affecting the taste of the food. The alloy, after polishing, obtains very good gloss, and its mechanical properties are comparable with the properties of the cobalt alloys. The hardness of the nickel-chromium alloys equals about 240 HV10, which allows their easy mechanical treatment with the use of appropriately selected tools [5-11].

Electrochemical corrosion behaviour of Ni-Cr-Mo dental alloys depends primarily on the Cr and Mo levels in an alloy [12]. In commercial alloys, the compositions of Cr and Mo usually range from 11% to 25% and from 0 to 10% (mass fraction),

\* AGH UNIVERSITY OF SCIENCE AND TECHNOLOGY, FACULTY OF METALS ENGINEERING AND INDUSTRIAL COMPUTER SCIENCE, MICKIEWICZA AV. 30, 30-059 KRAKÓW, POLAND

\*\* AGH UNIVERSITY OF SCIENCE AND TECHNOLOGY, FACULTY OF FOUNDRY ENGINEERING, REYMONTA ST. 23, 30-059 CRACOW, POLAND

<sup>#</sup> Corresponding author: jap@agh.edu.pl

respectively [13]. Both microstructure and casting defect have pronounced effect on the ion release in actual practice. The defects of dental cast alloys include mainly shrinkage porosity, inclusion, micro-crack and dendritic structure [14,15]. Only few reported works were available on the influence of casting procedures on the corrosion resistance of dental alloys [16,17].

Chromium is the main alloying element in Ni-based alloys and is added to promote the formation of a stable passive oxide layer that is highly resistant to corrosion. Molybdenum is also frequently added to promote resistance to pitting and crevice corrosion [18].

A disadvantage of the Ni-Cr-Mo alloys is the fact that a significant part of the population, where 5-10 times more often, it is the case of women than men, is allergic to nickel compounds. That is why nickel alloys, despite their positive advantageous mechanical properties and very good corrosion resistance, are more rarely used than the cobalt alloys.

In the presented study, the effect of the casting technology on the corrosion resistance of the Ni-Cr-Mo alloys was examined. The tests were conducted on the commercial alloy Argeloy N.P Be-Free (Ni-Cr-Mo) by Argen and the same alloy, yet remelted and cast by the lost mould method performed by a dental technician.

After the performed electrochemical tests, examinations of the surface of the investigated alloys were conducted by means of a scanning electron microscope with an X-ray microanalyser.

The aim of the tests was to compare the microstructural, X-ray diffraction and corrosion resistance properties in a solution of artificial saliva of the commercial Ni-22Cr-9Mo alloy, which, at the further stage of the research, was remelted and cast by the lost mould method.

The following tested series was performed on both the commercial alloy and the same alloy after remelting and re-casting.

## 2. Material and test methodology

One of the test samples was the commercial Ni-Cr-Mo alloy by the name of Argeloy N.P Be-Free, produced by Argen, in

the form of manufacture-prepared cylinders, 9 mm in diameter and 12 mm high. The chemical composition of the tested alloys are presented in Table 1. The physicochemical and mechanical properties of the Ni-Cr-Mo alloys declared by the producer are compiled in Table 2.

The next stage of the research was remelting the examined Ni-Cr-Mo alloy and casting it by a dental technician, by means of the precision casting technique (lost mould casting or lost wax casting), used for the product specification. The first step of the casting process was the preparation of a wax model for the alloy, 5 mm in diameter and 15 mm long. The following step was placing the wax model in a ring, which was then filled with a refractory mass based on phosphates. After casting, the ring was placed into the pressure chamber and the pressure of 0,4 MPa was applied for 20 minutes, with the aim of a proper binding of the refractory mass. After the mass had been bound, the formed crucible was placed into the furnace and the heating process began at the rate of 7°C/min.

Two isothermal holds were made during the heating. At the first one, at 250°C for 20 minutes, evaporation of the water and the wax from the casting ring took place. The second hold occurred at 600°C for the same time period, that is 20 minutes, when the silica transformation was observed. The finalization of the process took place at 950°C/20 min, and next, the casting process began in the Vulcan 3-550 furnace. After casting, the sample was removed from the furnace and cooled in open air.

The following step was removing the refractory mass and mechanical sand blasting by means of the Ecoblast Kombi machine, with 200 µm granularity sand and the pressure of 6 MPa. The last step of the sample preparation was a mechanical removal of the feed channel.

With the purpose of revealing the microstructure, metallographic specimens of the cross-sections were prepared, which were then chemically etched with the use of reagents consisting of 3 ml HNO<sub>3</sub> + 1 ml HF + 1 ml glycerin. The microstructure observations were performed with the use of the light microscope LEICA DM 4000.

The chemical composition microanalysis of the samples tested in respect of corrosion resistance were conducted by

TABLE 1

Chemical composition of tested alloy Ni-Cr-Mo [19]

Brand name	Alloy	Chemical composition, % weight							
		Ni	Cr	Mo	Ta	Nb	Fe	C	Mn
ARGELOY N.P BE-FREE	Ni-Cr-Mo	54	22	9	4	4	4	max. 1.5	max. 1.5

TABLE 2

Mechanical and physical properties of alloy Ni-Cr-Mo according to producer [19]

Mechanical properties		Physical properties	
Yield point $Re_{0.2}$ [MPa]	360	Density [g/cm <sup>3</sup> ]	8.6
Young's modulus [GPa]	160	Expansion coefficient thermal	14.1÷14.4
Hardness [HV10]	240	Melting point [°C]	1220÷1230
Extending A <sub>5</sub> [%]	6	Soaking heat [°C]	1220
		Temperature of pouring out [°C]	1370

means of the electron scanning microscope HITACHI S-3500N, equipped with an EDS analyzer by Noran. The analysis was made by the point-by-point method on the surface of the examined alloys. The analysis results have been presented in the form of characteristic X-ray spectra and the element contents have been determined. Also, X-ray diffraction tests were performed by means of the diffractometer D500 by Siemens, with monochromatic radiation of the copper-anode lamp  $\lambda_{K\alpha} = 1,54\text{\AA}$ . The conditions of the measurement were: angular step  $\Delta 2\theta = 0,02^\circ$ , time of counts  $\tau = 5\div 10$  s, angle measurement range  $2\theta = 30\div 100^\circ$ .

The surface of the electrochemical test-prepared alloy equaled respectively  $0,79\text{ cm}^2$  for commercial and  $0,20\text{ cm}^2$  for recast sample. Before the measurement, specimens of the Ni-Cr-Mo alloy were polished with the use of abrasive papers made of silicon carbide (SiC) with the granularity of up to 4000.

The chemical composition of artificial saliva solution includes: NaCl:  $0,400\text{ g/l}$ , KCl:  $0,400\text{ g/l}$ ,  $\text{CaCl}_2\cdot\text{H}_2\text{O}$ :  $0,795\text{ g/l}$ ,  $\text{NaH}_2\text{PO}_4\cdot\text{H}_2\text{O}$ :  $0,780\text{ g/l}$ ,  $\text{Na}_2\text{S}\cdot\text{H}_2\text{O}$ :  $0,005\text{ g/l}$ , urea:  $1,000\text{ g/l}$  [20]. The tests were carried out at  $37^\circ\text{C}$ .

The polarization tests were carried out within the potential range of  $-1,5\div 1,5\text{ V}$ , with rate of potential changes equaled  $1\text{ mV/s}$ . The measurements of the polarization curves were performed in a three-electrode system, where the auxiliary electrode was a platinum gauze, the working electrode was represented by

the examined alloys and the reference electrode was a Ag/AgCl in 3M KCl. The measurements were carried out with the use of a potentiostat VoltaLab PGZ301.

### 3. Analysis of the microstructure

The performed microscopic observations made it possible to reveal the microstructure of the examined commercial Ni-Cr-Mo alloy and the alloy cast by the lost wax method. Exemplary microstructural images are presented in Figure 1.

The microstructure of the tested nickel-chromium-molybdenum alloy was dendritic, typical of cast materials. According to the literature data [21,22], in the structure of the Ni-Cr-Mo alloy, the dendrites are constructed mainly of intermetallic phases  $\gamma$  (A1), enriched with nickel, and the increased content of molybdenum causes its segregation into the interdendritic areas. In the Ni-Cr-Mo alloys, no strong chromium segregation is observed, however, its content in the interdendritic areas is lower in comparison with the material base. The presence of such elements as Ta, Nb, Fe and C in the alloy also has an important effect on the final microstructure of the cast Ni-Cr-Mo alloy. These additions are accumulated in the interdendritic areas in the form of minor precipitations.

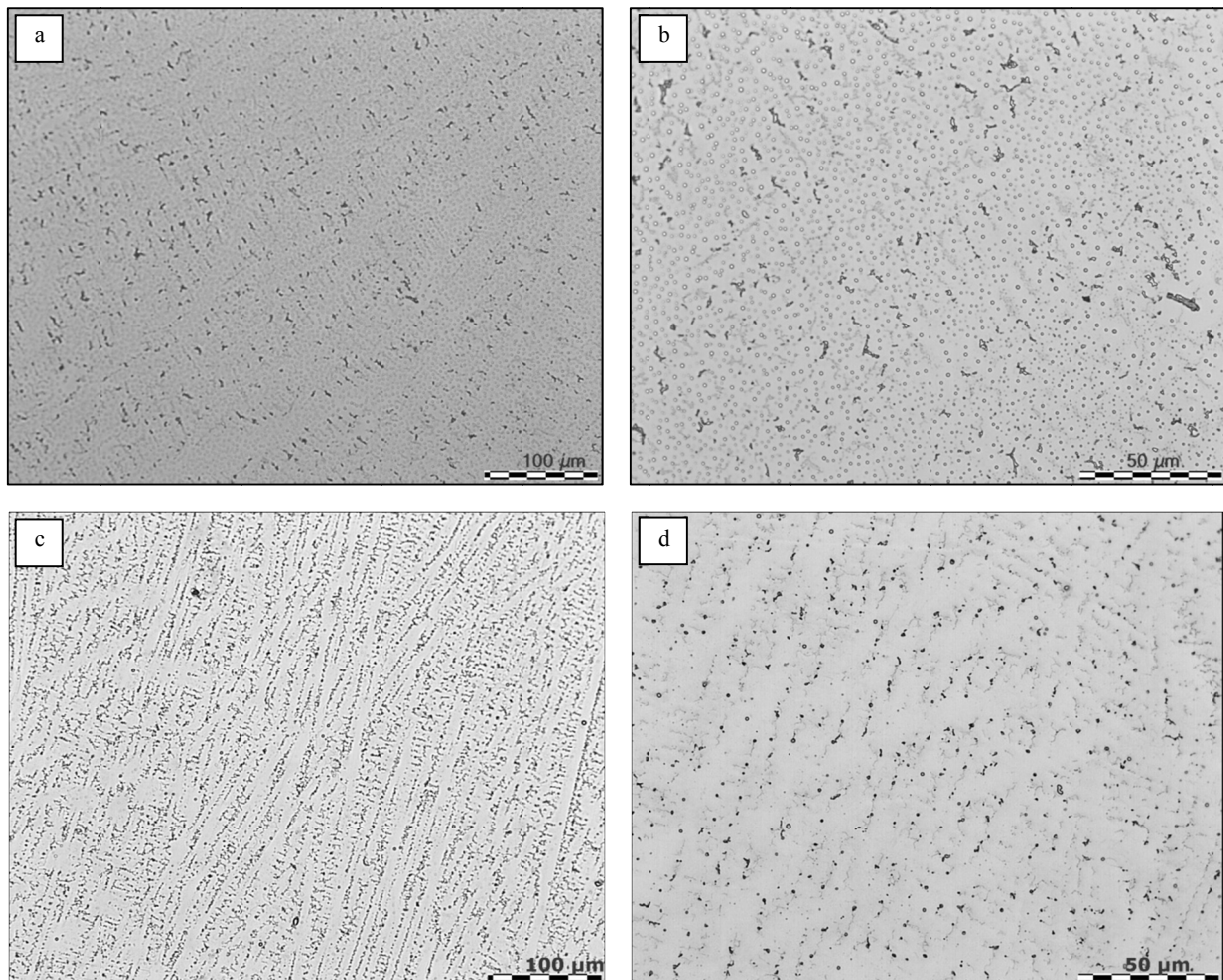


Fig. 1. Microstructure of Ni-Cr-Mo alloy; a÷b **commercial** alloy, c÷d **recast** alloy

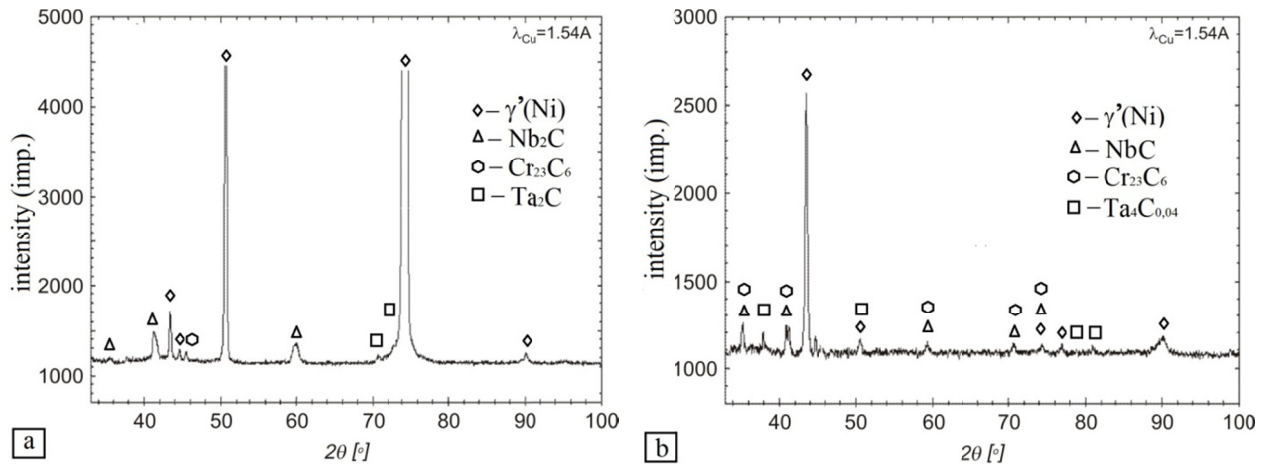


Fig. 2. X-ray diffraction of the phase qualitative analysis of alloy Ni-Cr-Mo, a) **commercial** alloy, b) **recast** alloy

#### 4. X-ray phase qualitative analysis

The X-ray diffraction phase analysis was performed in order to identify the phases present in the examined materials, and its results are presented in Figure 2.

The qualitative analysis performed for the Ni-Cr-Mo alloy showed a content of phase  $\gamma'$  (Ni) in the examined samples, as well as  $\text{Cr}_{23}\text{C}_6$  type carbides, and  $\text{Nb}_2\text{C}$ ,  $\text{Ta}_2\text{C}$  (commercial alloy) and  $\text{NbC}$ ,  $\text{Ta}_4\text{C}_{0,04}$  (cast alloy) phases (Fig. 2).

#### 5. Electrochemical tests results

##### 5.1. Open Circuit Potential

The open circuit potential of the alloys changes in the function of time. Figure 3 presents the change in the potential value of the examined alloys in time. The potential value was measured for the period of about 10 h. The value of the potential of the commercial alloy is much higher than in the case of the alloy re-cast by the dental technician. The potential value of the industrial alloy at the beginning of the measurement equaled  $-0,32$  V and it changed in time, constantly increasing its value till the moment when it reached about  $-0,15$  V after approximately 30000 s. The potential of the re-cast alloy equaled  $-0,25$  V at the beginning of the measurement. After about 8880 s, it reached a stable value equaled  $-0,26$  V. The obtained test results clearly demonstrate that the commercial alloy exhibits a significantly higher corrosion resistance than the recast alloy.

##### 5.2. Polarization and SEM/EDS analysis

As a result of the polarization tests, we obtained polarization curves presented in Figure 4. The examined materials characterize in similar courses of the obtained curves for the rate of the potential change equaling 1 mV/s.

The polarization curves made for the tested samples confirm the results of the open circuit potential tests, which demonstrate

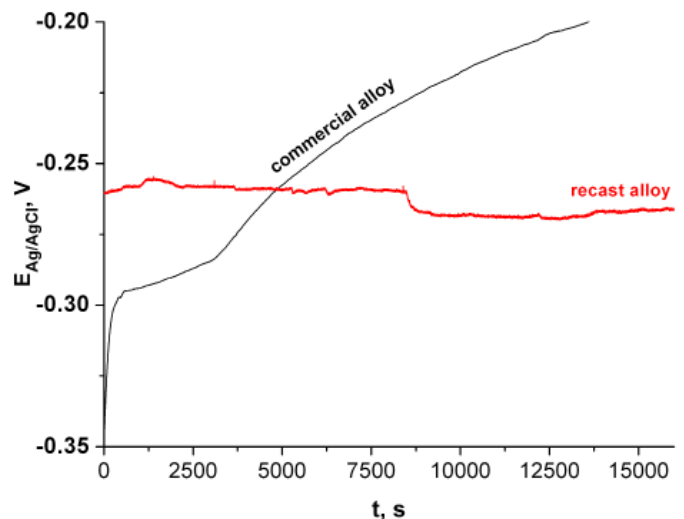


Fig. 3. Evolution of open circuit potential of tested alloy

that the commercial alloy characterizes higher corrosion resistance than the one recasted by the technician. The course of the polarization curves suggests that the examined dental alloy undergoes active dissolution, which is proved by the peak formed on the curve, very clearly seen on the commercial alloy.

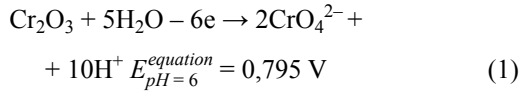
The anodic polarization curves suggest that the alloy, both before and after casting, easily undergoes passivation, which hinders the material dissolution. Above the potential ( $E_{a1}$ ), on the anodic curve for the commercial alloy, we can observe a gradual drop of anodic current density, which proves the material's transition into passivity. On both obtained curves we can observe a very wide plateau range ( $-0,337 \div 0,868$  V), which, for the commercial alloy, is minimally longer than in the case of the cast alloy, and it is in the potential range of:  $-0,375 \div 0,878$  V.

The protective layer formed on the metal surface, as the literature suggests, is mainly constructed of  $\text{Cr}_2\text{O}_3$  [23]. In the passive area, for the commercial alloy, the anodic current densities are much lower than for the cast alloy and they are at the level of about  $0,008$  mA/cm<sup>2</sup>, which can be regarded as a satisfactory low value, proving the good protective properties of the passive layer.



Above the potential  $E = 0,872$  V for the commercial alloy and  $E = 0,862$  V for the cast alloy can be seen an increase in the current density on the polarization curves.

The increase of the current density is a consequence of the trans-passivation of the formation soluble corrosion products at high levels of metal atom oxidation, e.g.  $\text{CrO}_4^{2-}$ ,  $\text{MoO}_4^{2-}$  (or solid  $\text{Ni}_2\text{O}_3$ ). Of all the three main alloy components, the most probable is the reaction of dissolution of the passive layer consisting mainly of chromium oxide (III) to  $\text{CrO}_4^{2-}$ :



The value of the equilibrium potential given in equation (1) corresponds to the case when the passive layer is constructed of the  $\text{Cr}_2\text{O}_3$  hydrate (hexagonal network) [9,24].

Passivation of Ni-Cr alloys is strongly connected with the presence of high level of Cr. Ni-Cr alloys with higher level of Cr (about 25%) exhibited superior corrosion resistance due to the more uniform distribution of Cr in the microstructure of alloy. The homogeneous distribution of Cr is critical especially in low-Cr nickel based alloys for better corrosion resistance. Compared with  $\text{Cr}_2\text{O}_3$ , the oxide of nickel is more porous and has less protective ability to corrosion [13].

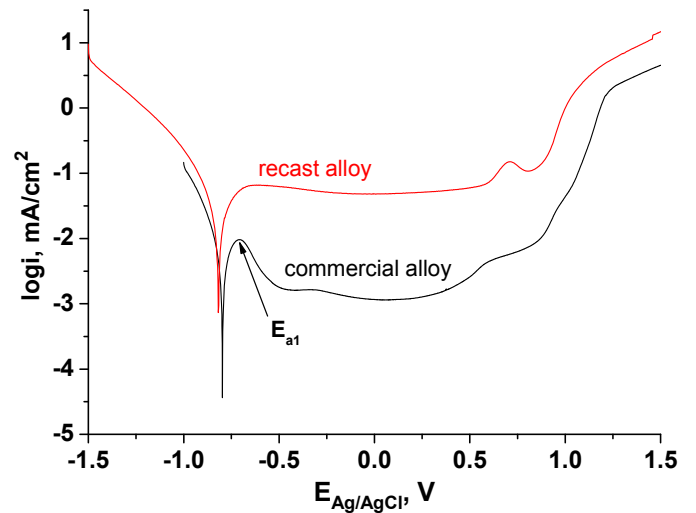


Fig. 4. Polarization curves of tested samples

The surfaces of the alloys after the potentiodynamic polarization experiment were examined using SEM to identify the sites of corrosion attack (Fig. 5). There is thick corrosion product layer on the investigated alloy. Such a layer is visible to the naked eye.

EDS line analysis of the corroded areas of both investigated samples indicates severe depletion (over four times) of

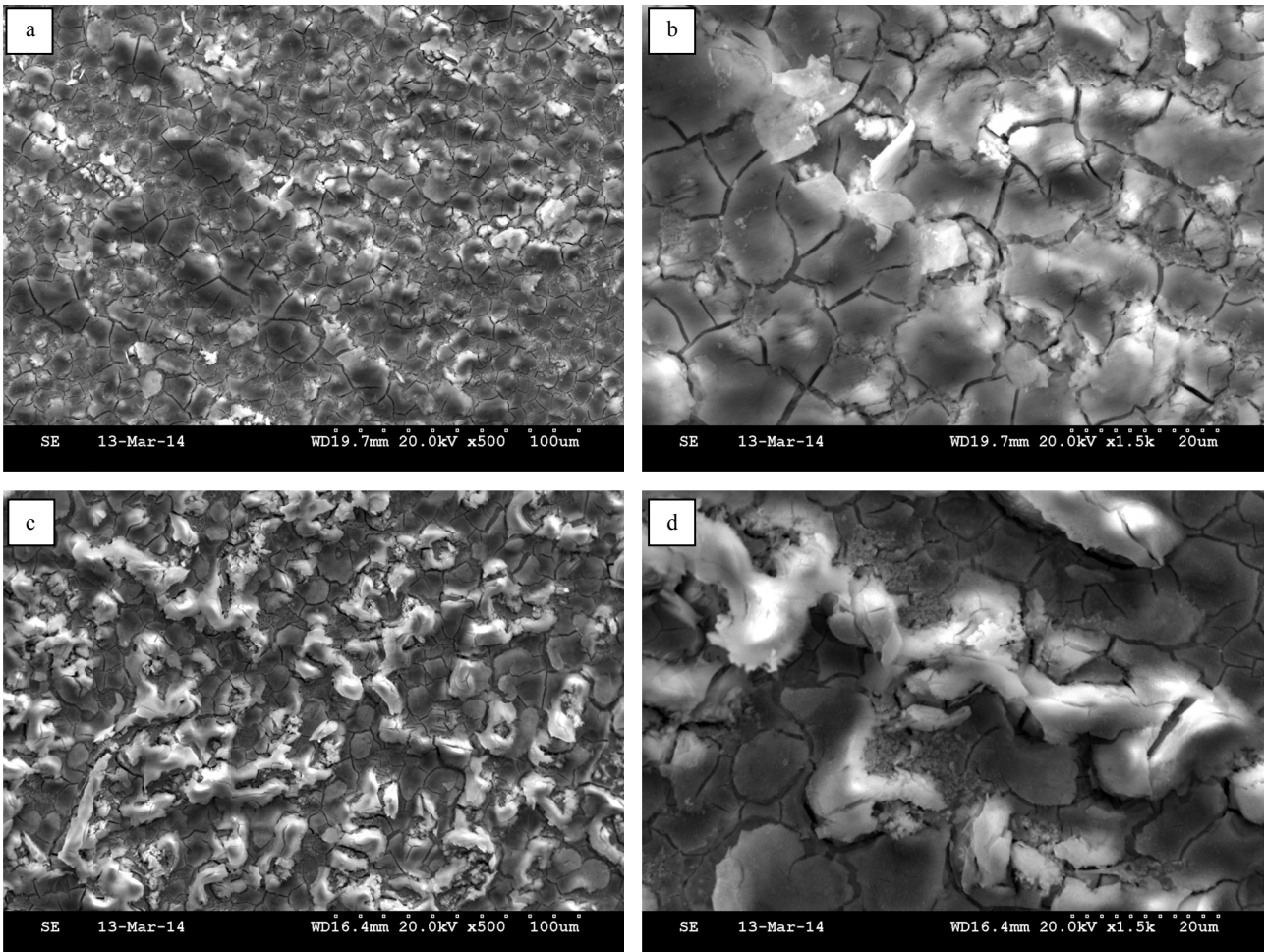


Fig. 5. SEM images of Ni-Cr-Mo alloy after polarization test; alloy; a=b commercial alloy, c=d recast alloy

nickel and chromium content (Fig. 6, point 1, Fig. 7, point 1). In Figure 6, in points 2, 3 and 4, we can see a non-uniform distribution of nickel and chromium in the potentiostatically formed layer on the commercial alloy.

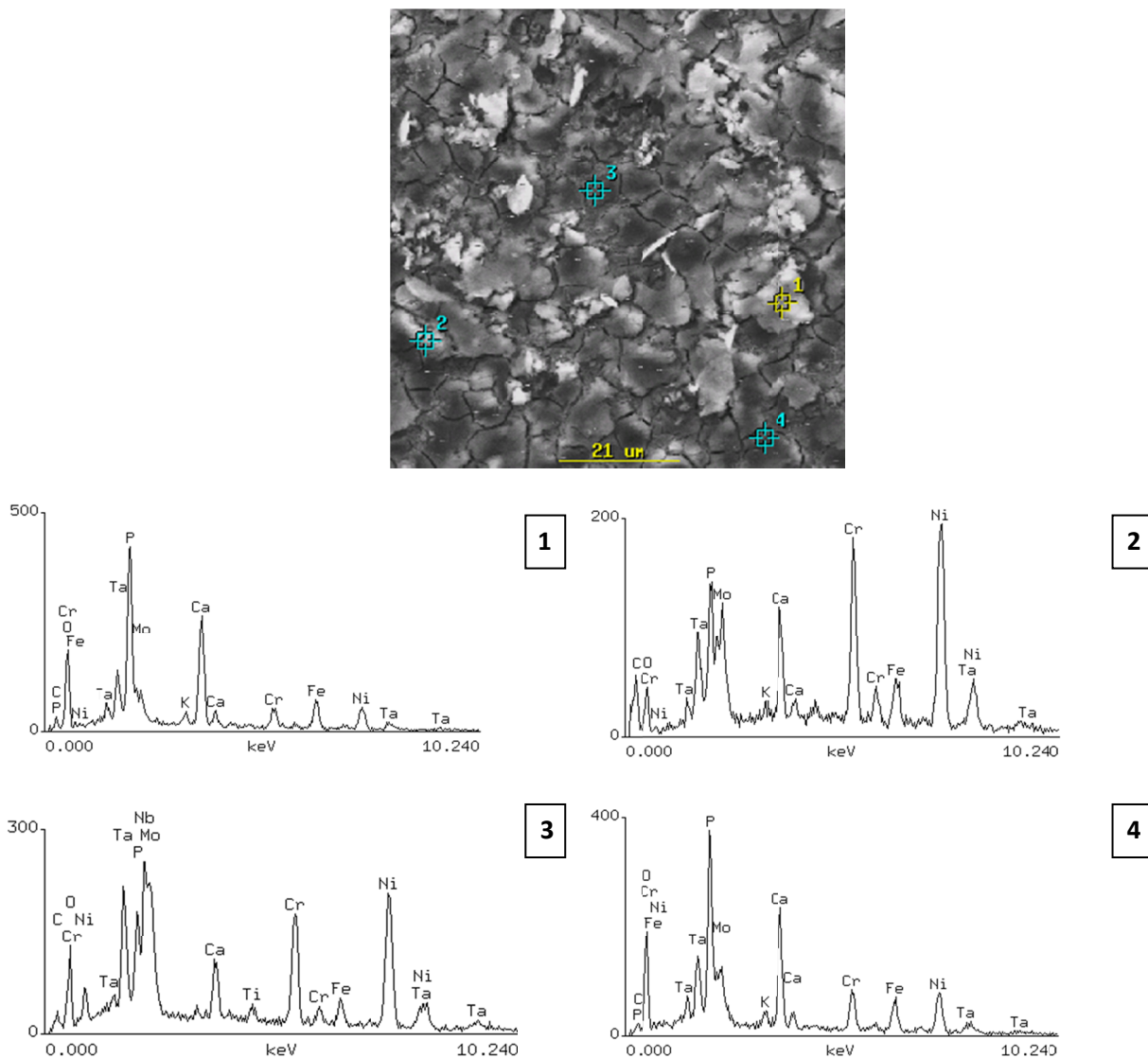
In the commercial alloy, we can see that, the content of Mo is constant and equals about 9% weight. Also, in Figure 6, in point 1, we can see a two-fold enrichment of the film with Fe, Nb and Ta.

Fig. 7, points 1, 2, shows an about 13-fold impoverishment in nickel and about 4-fold impoverishment in chromium. The Mo content in the formed film does not change as compared with the pure alloy, whereas the Nb and Ta contents increase about 3 times.

### 6. Summary and conclusions

The group of non-precious metal alloys currently used at dental prosthetics laboratories are the Ni-Cr-Mo alloys. The nickel-based alloys were introduced into prosthetics laboratories in the 80-ties of the twentieth century as materials replacing the costly precious metals (gold alloys), which were applied as a foundation for ceramic faced crowns.

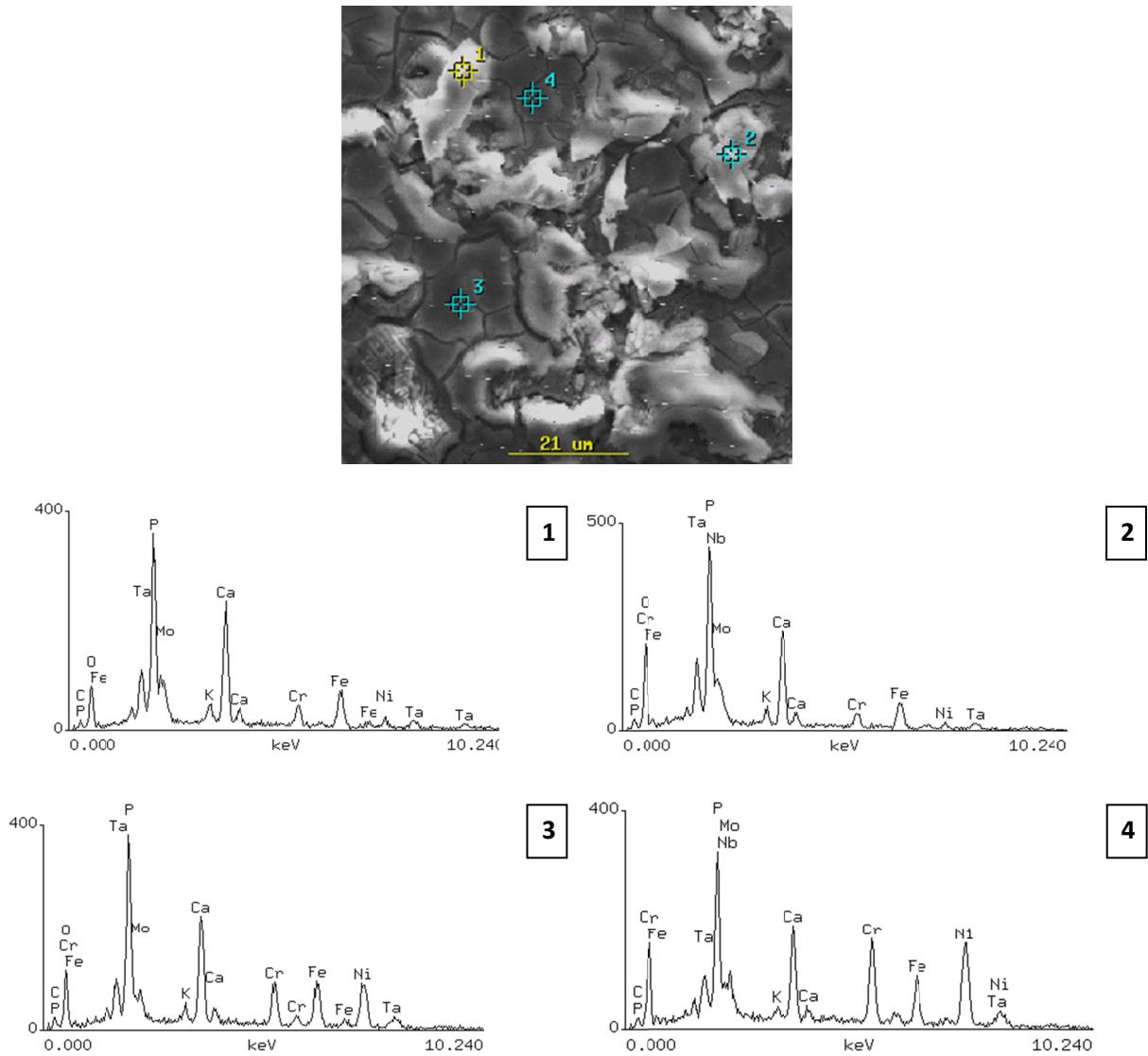
One of the advantages of the Ni-Cr-Mo alloys is their high modulus of elasticity as compared with the gold alloys. This allows the application of thinner cross-sections of the used alloy, and, in consequence, a lower degree of damage to the healthy tooth during the creation of the crown [25]. The coefficient of



Chemical composition of the precipitates observed in Ni-Cr-Mo alloy

Area	Chemical composition, % weight							
	Ni	P	Ca	Fe	Cr	Nb	Mo	Ta
1	12.87±1.45	20.96±1.50	19.77±1.25	10.85±1.70	5.29±0.66	9.27±0.66	9.02±1.73	11.97±3.28
2	40.85±2.97	5.33±0.55	5.22±0.40	6.00±0.82	15.84±1.26	7.92±1.73	9.01±1.37	9.74±3.86
3	32.82±1.67	4.32±0.63	4.00±0.35	3.90±0.68	13.08±0.63	18.40±2.07	12.58±1.75	10.91±3.13
4	18.95±1.70	14.97±1.63	16.22±1.19	9.86±1.06	9.53±1.25	10.02±2.93	10.99±1.87	9.45±3.67

Fig. 6. SEM image of Co-Cr-Mo commercial alloy and EDS spectrogram of areas shown in SEM image



Chemical composition of the precipitates observed in Ni-Cr-Mo alloy

Area	Chemical composition, % weight							
	Ni	P	Ca	Fe	Cr	Nb	Mo	Ta
1	4.03±1.10	19.95±0.95	18.23±0.81	15.18±1.32	5.43±0.73	12.61±2.83	8.64±1.88	15.95±3.86
2	3.60±0.98	21.99±0.95	19.83±0.79	14.32±1.92	5.64±1.16	13.18±2.98	9.66±1.98	11.77±3.43
3	22.89±1.85	16.87±0.78	16.30±1.12	14.85±1.21	10.75±1.25	4.82±2.22	7.14±1.43	6.39±3.56
4	32.86±2.75	12.42±0.68	9.45±0.49	10.77±1.59	15.77±1.25	4.82±2.01	7.95±1.39	5.97±3.26

Fig. 7. SEM image of Ni-Cr-Mo **recast** alloy and EDS spectrogram of areas shown in SEM image

thermal expansion of the nickel-based alloys is in accordance with the coefficient of thermal expansion of the ceramics used for facings, which, in consequence, during the burring of the metal-ceramic crown, ensures a tight joint of the metal with the ceramic material and prevents the facing from cracking [26].

What is more, it should be noted that, in the technology of making the prosthetic element, these alloys are easy to remelt by means of a gas-oxygen burner, which makes the Ni-Cr-Mo alloy to be commonly applied e.g. for permanent elements of crowns and bridges, constituting a good basis for dental porcelain firing [27].

The presented study undertakes materials engineering investigations of the Ni-22Cr-9Mo alloy. The test material was

a commercial alloy and the same alloy, remelted and re-cast. The tests aimed at examining the effect of the alloy's remelting on its microstructure and corrosion resistance in the environment of artificial saliva. Additionally, evaluation was made of the effect of the morphology of the passive layer on the corrosion resistance of the Ni-Cr-Mo alloy.

Based on the performed investigations, the following conclusions were drawn:

1. The metallographic tests of the solidified Ni-22Cr-9Mo alloy, both in the state as-delivered (commercial alloy) and after remelting, revealed a dendritic structure, the skeleton of which was constituted by dendrites of a branched tree-like structure.

2. It was observed that, in the microstructure of the Ni-Cr-Mo alloy, the dendrites were mainly constructed of the intermetallic phase  $\gamma'$  (FCC) enriched with nickel. The increased content of Cr and other elements, such as Nb and Ta, in the alloy, caused a strong segregation, and, in consequence, enrichment of the interdendritic areas in carbide precipitations of the MC,  $M_2C$  and  $M_{23}C_6$  type.
3. The electrochemical measurements suggest that the recast alloy characterized slightly lower corrosion resistance than the commercial alloy. The progress of the polarization curves is characteristic for high corrosion resistance materials.
4. SEM images and EDS line analysis of the corroded areas of both investigated samples indicates severe depletion of nickel and chromium content. On both investigated samples can be seen that enrichment of the layer with elements such as Fe, Nb, Ta caused strong segregation and enrichment in carbide precipitations of the MC,  $M_2C$  and  $M_{23}C_6$  type.

#### Acknowledgements

The work has been implemented within the framework of statutory research of AGH University of Science and Technology, contract No **11.11.110.299 AGH**

#### REFERENCES

- [1] ISO 6871-2:1994 Dental base metal casting alloys – Part 2: Nickel-based alloys (1994).
- [2] J. Geis-Gerstorfer, K. Passler, *Dental Materials* **9**, 3, 177-81 (1993).
- [3] L. Braga Alkmin, A.A. Araújo Pinto da Silva, C.A. Nunes, C. dos Santos, G.C. Coelho, *Materials Research* **17**, 3 (2014).
- [4] J. Bauer, J.F. Costa, C.N. Carvalho, RHM. Grande, AD. Louguericio, A. Reis, *Journal of Prosthodontic Research* **56**, 264-71, (2012).
- [5] H.H. Huang, *Journal of Biomedical Materials Research* **60**, 3, 458-465 (2002).
- [6] A. Eftekhari, *Applied Surface Science* **220**, 1-4, 343-348, (2003).
- [7] J. Augustyn-Pieniążek, A. Łukaszczyk, R. Zapala, *Archives of Metallurgy and Materials* **58**, 4, 1281-1285 (2013).
- [8] Q. Chen, G.A. Thouas, *Materials Science and Engineering* **87**, 1-57 (2015).
- [9] K. Radomska, D. Klimecka-Tatar, K. Jagielska-Wiaderek, *Corrosion Protection* **57**, 7, 262-268 (2014).
- [10] D. Klimecka-Tatar, *Metal* 2-6 (2015).
- [11] H-Y. Lin, B. Bowers, J.T. Wolan, Z. Cai, J.D. Bumgardner, *Dental Materials* **24**, 378-385 (2008).
- [12] M.D. Roach, J.T. Wolan, D.E. Parsell, J.D. Bumgardner, *Journal of Prosthetic Dentistry* **84**, 623-634 (2000).
- [13] C.M. Wylie, R.M. Shelton, G.J. Fleming, A. Davenport, *Dental Materials* **23**, 714-723 (2007).
- [14] A. Fossati, F. Borgiolo, E. Galvanetto, T. Bacci, *Corrosion Science* **46**, 917-927 (2004).
- [15] L. Reclaru, R.E. Unger, C.J. Kirkpatrick, C. Susz, P.-Y. Eschler, M.-H. Zuercher, I. Antoniac, H. Lüthy, Ni-Cr based dental alloys; Ni release corrosion and biological evaluation, *Materials Science and Engineering C* **32**, 1452-1460 (2012).
- [16] C. Mulders, M. Darwish, R. Holze, *Journal of Oral Rehabilitation* **23**, 825-831 (1996).
- [17] S.J. Kim, Y.M. Ko, H.C. Choe, *Advanced Materials Research* **15-17**, 164-168 (2007).
- [18] J. Loch, A. Łukaszczyk, J. Augustyn-Pieniążek, H. Krawiec, *Solid State Phenomena* **227** (2015).
- [19] www.argen.com
- [20] ISO 10271:2001 Dental metallic materials – Corrosion test methods (2001).
- [21] M.J. Perricone, J.N. Dupont, *Metallurgical and Materials Transaction A* **37A**, 1267-1280 (2006).
- [22] A. Korneva I. Orlicka, K. Sztwiertnia, G. Zaikov, *Chemistry & Chemical Technology* **8**, 1, 103-106 (2014).
- [23] E. Juzeliunas, K. Leinartas, J., *Solid State Electrochem* **6**, 302-310 (2002).
- [24] M. Pourbaix, *Lectures electrochemical corrosion*, PWN, Warszawa, (1978).
- [25] Ch.M. Wylie, R.M. Shelton, G.J.P. Fleming, A.J. Davenport, *Dental Materials* **22**, 714-723 (2007).
- [26] J.W. McLean, *The science and art of dental ceramics* **1**, Quintessence Publishing, Chicago, (1979).
- [27] H.H. Huang, M.C. Lin, T.H. Lee, H.W. Yang, F.L. Chen, S.C. Wu, C.C. Hsu, *Journal Oral Rehabilitation* **32**, 206-212, (2005).